IEEE Access
Multidisciplinary | Rapid Review | Open Access Journal

IEEE VEHICULAR TECHNOLOGY SOCIETY SECTION

Received April 6, 2021, accepted April 19, 2021, date of publication April 23, 2021, date of current version May 4, 2021.

Digital Object Identifier 10.1109/ACCESS.2021.3075324

An Adaptive Cell Selection Scheme for 5G Heterogeneous Ultra-Dense Networks

IBTIHAL AHMED ALABLANI [1,2] AND MOHAMMED AMER ARAFAH [1]

[1]Department of Computer Engineering, College of Computer and Information Sciences, King Saud University, Riyadh 11543, Saudi Arabia
[2]Department of Computer Technology, Technical College, Technical and Vocational Training Corporation, Riyadh 11472, Saudi Arabia

Corresponding author: Ibtihal Ahmed Alablani (438203904@student.ksu.edu.sa)

This work was supported by the Deanship of Scientific Research at King Saud University through the Research Group under Grant RG-1440-122.

ABSTRACT Fifth-generation (5G) cellular networks are a promising technology to meet the rapid growth in wireless traffic. Small cells are critical in fulfilling the requirements of 5G networks. A heterogeneous ultra-dense network (HUDN) is an enabling technology consisting of several types of small cells to enhance the performance of 5G networks effectively. A critical issue of HUDN is the cell selection method because the traditional technique for cell selection is inapplicable in such a network. This study proposes a novel adaptive cell selection (ADA-CS) scheme. It adapts to various characteristics of HUDNs and vehicle movements. It performs six phases to select the best base station with which to be associated. Simulation results show that, with low- and medium-speed vehicles, the ADA-CS scheme outperforms the traditional protocol in terms of the average number of handovers by 42.39%. In addition, it is superior to some relevant recent schemes by up to 36.53%. The adaptation feature of the proposed protocol provides additional improvements regarding the average number of handovers with high-speed vehicles. Therefore, it achieves superiority in terms of the average number of handover failures and unnecessary handovers. In addition, the ADA-CS scheme enhances the average achievable downlink data rates and spectral efficiency per vehicle by 3.98% and 2.79% compared with the traditional and the relevant recent schemes.

INDEX TERMS 5G, cell selection, 3GPP cellular networks, cone angle, handover, small cells, HUDNs, adaptive association.

I. INTRODUCTION

Fifth-generation (5G) technology allows sharing of data and accessing information anywhere and anytime for anyone and anything [1]. Various 5G technology requirements are needed to support many new services and application areas, such as smart transportation, smart cities, and the Internet of Things (IoT) [2]–[5]. 5G technology will provide high data rates, energy efficiency, ultra-high reliability, extremely low latency, and fully connected coverage [6]. To fulfill these requirements, key enabling technologies have been identified, such as massive multiple-input multiple-output (mMIMO), millimeter wave (mmWave), and heterogeneous ultra-dense network (HUDN) techniques [3], [7], [8]. Nowadays, wireless cellular networks are denser and many issues must be addressed [9]. In the coming years, the prediction is that the number of deployed small cells will increase exponentially [10], [11]. An ultra-dense network (UDN) is defined by A. Gotsis *et al.*in [12] as a network where the number of small cells is greater than the number of active user equipments (UEs) [13]. An UDN is defined in [14]–[17] as a wireless network in which the density of small cells is high, which means around 600 active users per km^2. HUDNs involve very dense, low-power, small cells, such as picocells and femtocells, and high-power legacy macro-cells [6].

There are more advantages of deploying dense small cells in legacy micro-cells than in conventional networks. The distance between a user and the serving base station (BS) will be small, resulting in high signal strength and, therefore, high capacity. Users can deploy small cells, and the cost of deployment will be decreased. Load balancing, which means distributing incoming network traffic among cells, can be achieved. The problem of blind- spot coverage holes in macro-cells in 3G and 4G networks can be completely solved. The configuration of small cells is flexible, and by setting intelligent rules, interference can be decreased, and

The associate editor coordinating the review of this manuscript and approving it for publication was Jie Gao.

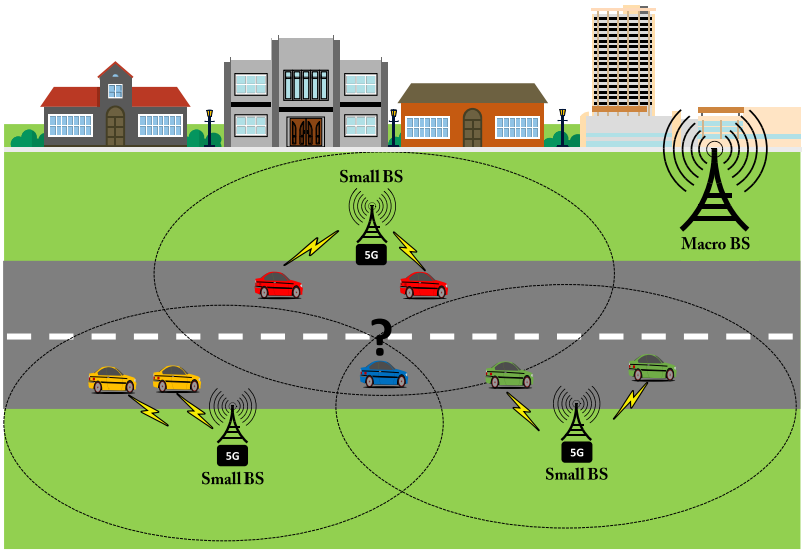

FIGURE 1. Cell selection issue in HUDNs.

energy efficiency can be improved [1], [18], [19]. Spectral efficiency can be enhanced through efficient spectrum use by reusing frequencies over relatively small distances [20], [21]. However, because of ultra-dense deployment and the uncertainty of user deployment features, HUDNs face challenges, such as radio resource allocation, cell selection, and interference mitigation [18], [19]. Furthermore, increasing the density of the BSs will increase the average number of handovers (HOs), leading to significant signaling traffic overhead for moderate-to-high-speed users [22].

Cell selection refers to determining a BS to which UE will be connected [23]. As defined in the third-generation mobile partnership project (3GPP) technical specification, cell selection includes selection, reselection, and handover [24]. In Long Term Evolution (LTE) and beyond, handover techniques are classified into hard and soft handover (HO). In hard HO, the connection to the serving BS is broken before the connection to the target BS is made, while soft HO makes the connection before breaking [25]. In HetNets, there are two types of HOs; namely, vertical HO (VHO) and horizontal HO (HHO). VHO occurs between heterogeneous BSs, while HHO happens between homogeneous BSs [26]. The traditional cell selection scheme is based on received signal strength (RSS) indicators (RSSI). In 5G HUDNs, this method is inapplicable because of high-density heterogeneous cells, which lead to complex interference and asymmetry of load distribution [3], [27]. Cell selection and handover triggering are still tricky problems [28]. Considering only one criterion, the RSSI, could lead to unbalanced network loads, inefficient handovers, and service interruptions [29]. Cell selection is critical in improving the load balancing, spectrum efficiency, and energy efficiency of 5G cellular networks [7]. Furthermore, cell detection and cell access times must be decreased to satisfy the low latency requirements. Therefore, improving a proper cell selection algorithm for 5G heterogeneous networks (HetNets) is challenging [30].

In 5G HUDNs, different coverage areas and densities of deployed cells exist [31]. Furthermore, vehicles travel on roads that have varying associated features, such as speed limits, lane widths, and traffic volumes [32], [33]. In addition, road vehicles vary in velocity and direction, depending on the driver's path and driving behavior. Because of these differences, there is a high probability that a non-ideal BS will be selected. A non-ideal BS leads to a ping-pong effect or failure in handover [34]. The ping-pong effect means that the number of handovers in a specific period exceeds a threshold [35]. Figure 1 displays the cell selection issue in an HUDN where a blue car should determine a BS to associate with, and signal strength indicators are insufficient to select the best BS.

Most of the existing works use static and non-adaptive methods to select cells. Adaptation can be performed by pre-defining a set of thresholds to change the selection strategy based on the characteristics of the vehicles and the network environment. In HUDNs, the macro BS tier is still required for high-speed vehicles, while the small BS tier is used by low- and medium-speed vehicles [36]. Recent works give high priority to BSs that have the strongest RSSI values and low or no priority is given for dwell time in a cell. In addition, there is a failure to include all the important selection factors, i.e., RSSI, speed, direction, and load; recent works depend on some factors and neglect others. In this work, we propose a novel adaptive cell selection (ADA-CS) scheme for 5G HUDNs that can adapt to different features of HUDNs and vehicles. In addition, it considers all important cell selection factors, with the best cell chosen carefully in order to stay connected with a serving BS as long as possible. In general, the main contributions of this study are to:

1) propose a novel adaptive cell selection scheme designed for 5G HUDNs, called ADA-CS. It can adapt to various features of vehicle movements and HUDNs specifications. It has six phases to select the best-associated BS.
2) evaluate the performance of the proposed ADA-CS algorithm using the MATLAB 2020a software. The evaluation was achieved in terms of the average (a) number of handovers; (b) dwell time within a serving cell; (c) number of handover failures (HOF); (d) number of unnecessary handovers (UHO); and (f) achievable downlink data rates and spectral efficiency. Various scenarios are considered in this study to prove the effectiveness of our ADA-CS scheme, using several simulation parameters. The simulation results show that the proposed scheme outperforms the traditional RSSI-based cell selection scheme. In addition, it achieves improvements over Kapoor *et al.*'s schemes.
3) study the impact of small cells density on the performance of a heterogeneous ultra-dense network.

The remainder of this study is arranged as follows. Section II presents recent studies on cell selection for 5G networks and their limitations. The proposed cell selection scheme and the system model are described in detail in Sections III and IV. Section V explains the results and discussion about the proposed cell selection strategy. Section VI concludes the paper.

Lists of the main notations and all abbreviations used in this paper are shown in Tables 1 and 3, respectively.

TABLE 1. List of main notations.

Notation	Description
$\mathcal{B}$	Set of all macro and small BSs
$\mathcal{V}$	Set of all vehicles
i	Vehicles index
j	BSs index
n	Number of BSs
m	Number of vehicles
$\mathcal{A}$	Matrix of association variables between vehicles and BSs
a_{ij}	Association variable between vehicle i and BS j
$\hat{S}$	Speed threshold
$\hat{R}$	RSSI threshold
$\hat{L}$	Load threshold
θ_c	Cone angle
$PL_{UMa-NLOS}$	Path loss of urban macrocell environment without line-of-sight
$PL_{UMi-LOS}$	Path loss of urban microcell environment with line-of-sight
f_c	Carrier frequency
d	Distance between a vehicle and a BS
h_V	Vehicle height
h_{BS}	Base station height
h_E	Effective height
d'_{BP}	Breakpoint distance
c	The velocity of light in free space (3 x 10^8 m/s)
C	Length of a circle chord
σ_{SF}	Standard deviation of shadow fading
p_{tx}	Transmitted power from base station
h	The channel gain
$\zeta_{ij}(d)$	Path loss from base station j to vehicle i
γ_{ij}	SINR received by vehicle i from BS j
δ^2	The additive white Gaussian noise power
N_0	Noise power spectral density
BW	Subchannel bandwidth
r_{ij}	Achievable downlink data rate of vehicle i served by BS j
η_{ij}	Spectral efficiency of vehicle i served by BS j
N_i	Number of handovers of vehicle i
τ_i	Handover latency to move into a cell
τ_o	Handover latency to move out of a cell
R	Radius of cell
s	Speed of vehicle
P_{HOF}	Probability of handover failures
P_{UHO}	Probability of unnecessary handovers
N_{HOF}	Number of handover failures
N_{UHO}	Number of unnecessary handovers
N_{HO}	Total number of handovers
T_1	Time threshold of handover failure
T_2	Time threshold of unnecessary handover

II. RELATED WORK

This section presents some of the most relevant recent studies on cell selection for 5G networks. Cell selection studies differ regarding scope, performance metrics, mobility information awareness, problem-solving methods, and the number of simultaneous BS associations. Mobility information, such as movement velocity and direction, is a basis for many applications.

In [37], Moon and Cho proposed a movement-aware vertical HO strategy called modified RSS (RSS$-\alpha$). The handover decision is based on RSSI values and a combination factor (α). Numerical results demonstrate that RSS$-\alpha$ enhances the system performance in terms of the probability of assigning mobile stations to femtocells with the same number of HOs [38]. Habibzadeh *et al.* proposed a decision-making handover algorithm for HetNets in [39]. The decision is made based on the received signal strength and the traffic metric. The proposed scheme aims to enhance the probability of femtocell BS assignment and to reduce the number of unnecessary handovers. Simulation results demonstrate that the proposed strategy outperforms the conventional RSS$-\alpha$ algorithm. In [40], Habibzadeh *et al.* introduced two traffic-aware spectrum handover (SHO) approaches for cognitive HetNets. These approaches are called shared-to-reserved (SR) and reserved-to-shared (RS) and they are based on the channel reservation concept. Numerical results show that the proposed schemes outperform the existing works in terms of effective throughput, energy efficiency, blocking probability of primary users and forced termination probability of cognitive secondary users.

In [23], Goyal *et al.* improved an optimal cell selection strategy for mmWave networks. The research concluded that a user associates with one BS when there is minimal or no reallocation cost. A user will connect to many BSs simultaneously when the handover cost is high. Simulation results indicate that the proposed strategy has the highest average throughput per UE compared with the other schemes. In [41], the problems of joint user association, throughput maximization, and power allocation are presented in H-CRANs. An outer approximation approach (OAA) based on linear programming is used to simplify the NP-hard problem. Simulation results demonstrate that when the number of admitted users increases, the system's throughput will increase. Cacciapuoti introduced a user association strategy for mmWave networks in [42]. It overcomes the limitations of the traditional RSS-based association by considering load balancing and handover reduction. Furthermore, it consid-

ers dynamic changes in the network topology caused by UE movements.

Chen *et al.* proposed a novel virtual small cell selection approach in [43]. It depends on the pattern search to increase the ergodic sum rate of all mobile stations. Simulation results show that the proposed selection approach has lower computation complexity than a reference scheme. In [44], Elkourdi *et al.* proposed a cell selection algorithm based on the Bayesian game approach. This algorithm improves the network performance regarding latency minimization and the probability of proper cell association as a function of traffic type. Simulation results demonstrate that the proposed algorithm can achieve the 5G latency requirement with a probability exceeding 80%.

In [45], Gharam *et al.* introduced a cell selection strategy for 5G HetNets. It uses a non-cooperative game theory with two players, representing UE and BS. Simulation results show the effectiveness of the proposed strategy in minimizing users' blocking rate and improving the performance of 5G HetNets. Alyaei *et al.* proposed a hard flexible cell association scheme in [46] for non-uniform HetNets. The proposed scheme depends on the location of users, and the cell region is divided into inner, annular, and outer regions. In the inner and outer regions, hard cell association is applied. In the annular region, flexible cell association is used. Analytical results proved that coverage and user throughput are significantly enhanced.

In [3], Waheidi *et al.* proposed a user-driven multiclass cell association algorithm. Two classes of devices are considered in this work; namely, UE and low-power IoT devices. It uses the multi-armed bandit (MAB) game to solve the cell association problem. The performance results show that the throughput and energy efficiency are within 10% of the centralized solution. If there is mobility, the values will increase by <5%. In [1], Lei *et al.* proposed a user association and power control scheme for HetNets. The scheme was evaluated for delay and total transmit power minimization. The simulation results confirm that the proposed approach outperforms existing schemes under various system parameters.

Alizadeh *et al.* proposed a new user association scheme for mmWave MIMO networks in [47]. The problem was formulated as a mixed-integer nonlinear programming problem. An algorithm called worst-connection swapping (WCS) was designed to solve the user association problem. The simulation results demonstrate that the proposed approach enhances the network performance regarding load balancing through moving the traffic from heavy-loaded BSs to non-congested ones.

Lee *et al.* introduced a software-defined network (SDN)-based handover scheme in [48] to fulfill the latency requirement of 5G networks at <1 ms. It considers the mobility information of UE. The SDN controller calculates the next cell based on collected information using the linear programming problem-solving technique. The simulation results proved that the SDN-based scheme could find a cell with strong signal strength, low cell load, and long sojourn time based on the movement direction. In [49], Wickramasuriya *et al.* proposed a cell selection method that uses a recurrent neural network (RNN) to predict the next BS. A group of RSS values trained the RNN. The simulation results confirm that the proposed scheme can predict the optimal cell with an accuracy of over 98%.

In [50], Fan and Ansari proposed a throughput-aware and green-energy-aware user association algorithm for HetNets, called TAGE. An energy-throughput coefficient α is used to manage the trade-off between the throughput and on-grid power consumption. Simulation results show that TAGE enhances the effective throughput and conserves on-grid energy. Xu, Zheng, and Tang in [51] introduced an energy-aware user association method based on a matching-coalition game. It is designed for non-orthogonal multiple access (NOMA)-based mobile edge computing (MEC) networks. Simulation results show that the proposed scheme is superior to other simplified schemes in terms of minimizing energy consumption.

Kiishida *et al.* proposed a cell selection approach for 5G multi-layered radio access networks (RANs) in [24]. It considers the UE movement direction and velocity to decrease the number of frequent handovers. The simulation results proved that the proposed approach achieved an approximate 30% improvement in the number of handovers while maintaining the average flow time. In [34], Kapoor *et al.* proposed four mobility-aware cell selection schemes for a 5G ultra-dense small cell urban vehicular network. These schemes are called the minimum distance (MD), next neighbor on the same street (NN-S), next neighbor on the opposite street (NN-O), and the minimum load (ML). The cell selection problem was solved on the basis of the k-nearest neighbor (KNN) algorithm and the azimuth angle. The MD and ML schemes aim to select a small BS from the k-nearest neighbor list that has the minimum distance and minimum load, respectively. The NN-S and NN-O approaches target a small BS in the list that has the maximum azimuth angle in the range $[0,\pi/2]$, and the minimum azimuth angle in the range $[\pi/2,\pi]$. With low-speed vehicles, simulation results show that the MD approach has the highest handover rate compared with the other methods.

In [52], two modified weighted methods of the Technique for Order Preference by Similarity to Ideal Solution (TOPSIS) were proposed. These methods are called Proposed Entropy TOPSIS (PE-TOPSIS) and Proposed Standard Deviation TOPSIS (PSD-TOPSIS). They aim to manage the handover process in heterogeneous networks using multiple criteria; namely, SINR, Time of Stay (ToS), and the angle between a BS and UE trajectory. To weight the attributes for making a handover decision, the PE-TOPSIS uses the entropy weighting technique, while the PSD-TOPSIS is based on a standard deviation weighting technique. Simulation results show that the proposed schemes are superior to the existing methods in terms of the number of frequent handovers and radio link failures. Furthermore, they improve the achieved average user throughput.

The Multi-Connectivity-based User Association Algorithm (MCUAA) is proposed in [53] for 5G H-CRANs. This is a polynomial time heuristic algorithm that depends on Linear Programming Relaxation-Rounding (LPR-R) and Generalized Assignment Problem (GAP) heuristics. Simulation results prove that the proposed algorithm outperforms the existing methods in terms of power consumption, achievable rate, and time complexity.

Sun *et al.* in [54] developed two strategies to manage handovers in HUDNs, called movement-aware coordinated multipoint handover (MACH) and improved MACH (iMACH). MACH depends on the dwell time, while iMACH is based on the dwell time and the nearest BS. Simulation results demonstrate that the proposed methods outperformed the existing strategies in terms of handover probability minimization, coverage probability and throughput enhancements.

The recent cell selection studies presented in this section have the following limitations:

- All works use non-adaptive cell selection strategies to select an associated BS. Therefore, the existing cell selection methods depend on fixed methods to select cells. Adaptation can be implemented via pre-setting some thresholds to switch between cell selection schemes, since there are different tiers in HUDN environments.
- Most recent studies give high priority to the closest BSs that have the strongest RSSI values. On other hand, the dwell time in a cell takes low or no priority in selection of cells.
- Not all the important cell selection factors are included. For example, the load balancing issue is considered in some studies and these studies neglect other selection factors, such as the speed of a vehicle.
- Some works are designed for specific topologies and applying them to another environment leads to frequent handovers.

Therefore, there is an urgent need for an adaptive cell selection algorithm that can adapt to various characteristics of vehicles and HUDNs. The adaptive scheme is a strategy that can select a cell dynamically, not statically, based on some thresholds to enhance the performance of HUDNs. In addition, all cell selection factors should be considered in such a way as to choose the best cell. Furthermore, a cell selection algorithm should be applicable for applying for different HUDN topologies.

III. PROPOSED CELL SELECTION STRATEGY

In a conventional handover process, a user vehicle periodically scans the signal strength of all neighboring BSs to determine the most appropriate BS to associate with [55]. Only one criterion in HUDN leads to frequent HOs, unbalanced network loads, and service interruptions, which affect overall network performance [29], [34], [56]. To address this issue, this study proposes an adaptive cell selection scheme (ADA-CS) for vehicles in HUDNs that considers multiple criteria when selecting a cell. It refers to a scheme that can adapt to distinctive characteristics of HUDNs and vehicle movements.

A. MAIN FEATURES OF ADA-CS SCHEME

The main features of our ADA-CS strategy are:

- It adapts to different characteristics of vehicles and BSs to choose the appropriate cells by setting some predefined thresholds. In HUDNs, macro BSs are still required for high-speed vehicles [36]. On the other hand, low and medium speed vehicles can associate with small cells to benefit from their advantages.
- It selects cells that have the longest dwell times based on the directions and speeds of vehicles and by narrowing the selection process, using a cone angle. The closest cells that have the highest RSSI are not given a high priority.
- It considers all the important cell selection factors; namely, RSSI, the speed and direction of the vehicle, and cell loads. A small BS that has a high load will not be chosen, because the load distribution among small cells is important to improve the QoS and to enhance system capacity [57].
- The ADA-CS algorithm is applicable to different HUDN topologies, where it is designed to be suitable for different cell distributions and sizes.

B. CELL SELECTION PHASES

Macro and small BSs are represented by $\mathcal{B}_{macro}$ and $\mathcal{B}_{small}$, respectively. All BSs are denoted by $\mathcal{B} \in \{b_1, b_2, \ldots, b_n\}$. Distributed vehicles are represented by $\mathcal{V} \in \{v_1, v_2, \ldots, v_m\}$. The association variable between vehicle i and BS j is denoted as a_{ij}. A user vehicle can only be associated with one BS at a time. $\mathcal{A} \in \{a_{11}, a_{12}, \ldots, a_{ij}\}$ shows the vehicle association variable between vehicle i and BS j. If vehicle i is associated with base station j, $a_{ij} = 1$, otherwise $a_{ij} = 0$.

The proposed scheme has six main phases, as shown in figure 3, which are

1) **Configuration phase:** The configuration information is set in this phase, which includes the values of speed threshold ($\hat{S}$), RSSI threshold ($\hat{R}$), load threshold ($\hat{L}$), and cone angle (θ_c).
2) **Decision-making phase:** The decision is made on the basis of the vehicle's speed. If the vehicle's speed is greater than the speed threshold, which was set in the previous phase, the decision will be selection from the macro BSs as shown in equation (1).

$$X_1 = \{b_j | b_j \in \mathcal{B}_{macro}\}, \quad \forall\, v_i \in \mathcal{V} \; with \; s_i > \hat{S} \quad (1)$$

If the vehicle's speed does not exceed the speed threshold, the decision is to select from a small BSs as illustrated in equation (2).

$$X_1 = \{b_j | b_j \in \mathcal{B}_{small}\}, \quad \forall\, v_i \in \mathcal{V} \; with \; s_i < \hat{S} \quad (2)$$

Therefore, the decision at the end of this phase is between two possible selections; the macro or small BSs.

3) **Filtering phase:** This phase depends on the decision made in the previous stage. The RSSI values of the neighboring stations, whether they are macro or small BSs, are calculated according to the decision. If the decision is to select from the macro BS, single filtering is applied to the macro BS based on the RSSI threshold as described in equation (3).

$$X_2 = \{b_j | b_j \in X_1 \ \& \ RSSI_{ij} > \hat{R}\} \tag{3}$$

However, dual filtering is applied if the decision is to select from the small BSs. The first filter is based on the RSSI threshold (equation (3)), whereas the second filter depends on the load threshold (equation (4)). Therefore, small BSs with a load higher than $\hat{L}$ will not be selected, to avoid the blocking probability caused by exceeding the cell's capacity and to maintain the system performance.

$$X_3 = \{b_j | b_j \in X_2 \ \& \ L_j < \hat{L}\} \tag{4}$$

4) **Narrowing phase:** This phase is based on the value of the cone angle that was set in the configuration phase. The selection is narrowed to the BSs within the cone angle, depending on the vehicles' azimuths. This phase excludes remote BSs and BSs that are not located in the vehicle's direction (equation (5)).

$$X_4 = \{b_j | b_j \in X_3 \ \& \ b_j \ within \ \theta_c\} \tag{5}$$

5) **Selecting phase:** One BS is chosen to be associated with. If the decision in the decision-making phase is to choose from the macro BS, the macro BS with the largest RSSI value will be chosen, as shown in equation (6).

$$X = \{b_j | b_j \in X_2 \ \& \ b_j \ has \ max(RSSI_{ij})\} \tag{6}$$

However, if the decision is to choose from the small BS, the small BS within the cone angle and with the minimum angle relative to the vehicle's current location will be chosen (equation (7)).

$$X = \{b_j | b_j \in X_4 \ \& \ b_j \ has \ min(\theta_{ij})\} \tag{7}$$

6) **Handover triggering phase:** The handover is triggered based on the predefined RSSI threshold $\hat{R}$ and the signal power received by a vehicle i from the serving BS j. The HO trigger condition that should be fulfilled is defined in equation (8).

$$RSSI_{ij} < \hat{R}, \quad \forall \ b_j \in \mathcal{B} \ \& \ v_i \in \mathcal{V} \tag{8}$$

The pseudocode for the proposed adaptive cell selection scheme is presented in Algorithm 1.

Let us take an example of the proposed cell selection strategy (Figure 2). This example has a single macro BS and a high-density small BS. In the configuration phase, the configuration information is set. The thresholds of speed, RSSI, and loads are assumed to be 120 km/h, -80 dBm, and 90%, respectively. The vehicle's speed is 80 km/h, and the azimuth between a vehicle's direction and north is 45°. The cone angle is assumed to be 90°. In the decision-making phase, the vehicle's speed is compared with the speed threshold. If it does not exceed it, as in this example (80 km/h < 120 km/h), a decision is made to select a small BS. In the filtering phase, the small BSs are first filtered by removing small BSs with RSSI below the threshold (Figure 2a). Further filtering is done on the basis of the cells' loads (Figure 2b), where small BSs with a load higher than the load threshold (90% in this example) will be excluded. In the narrowing phase, the selection will be narrowed to those small BSs inside the cone angle (90° in this example), (figure 2c). The selection phase is where one small BS is selected that has the lowest azimuth between it and the vehicle direction (Figure 2d). Handover is triggered when the RSSI of the serving small BS is lower than a pre-defined threshold.

Algorithm 1: Pseudocode for the Proposed Adaptive Cell Selection Scheme

input : $\mathcal{B}_{macro}$; $\mathcal{B}_{small}$.
output: X.
========== Configuration Phase ==========
Set $\hat{S}$, $\hat{R}$, $\hat{L}$;
Set θ_{Cone};
for *i =1:m* **do**
  ======= Decision-Making Phase =======
  if $s_i > \hat{S}$ **then**
    $X_1 = \{b_j | b_j \in \mathcal{B}_{macro}\}$;
  else
    $X_1 = \{b_j | b_j \in \mathcal{B}_{small}\}$;
  end
  ========== Filtering Phase ==========
  $X_2 = \{b_j | b_j \in X_1 \ \& \ RSSI_{ij} > \hat{R}\}$;
  if $X_1 == \mathcal{B}_{small}$ **then**
    $X_3 = \{b_j | b_j \in X_2 \ \& \ L_j < \hat{L}\}$;
    ======== Narrowing Phase ========
    $X_4 = \{b_j | b_j \in X_3 \ \& \ b_j \ within \ \theta_c\}$;
  end
  ========= Selecting Phase ==========
  if $X_1 == \mathcal{B}_{macro}$ **then**
    $X = \{b_j | b_j \in X_2 \& b_j \ has \ max(RSSI_{ij})\}$;
  else
    $X = \{b_j | b_j \in X_4 \ \& \ b_j \ has \ min(\theta_{ij})\}$;
  end
  ==== Handover Triggering Phase =====
  if $RSSI_{ij} < \hat{R}$ **then**
    TriggerHO;
  end
end

C. CELL SELECTION CONSTRAINTS

There are some constraints that restrict vehicle association:

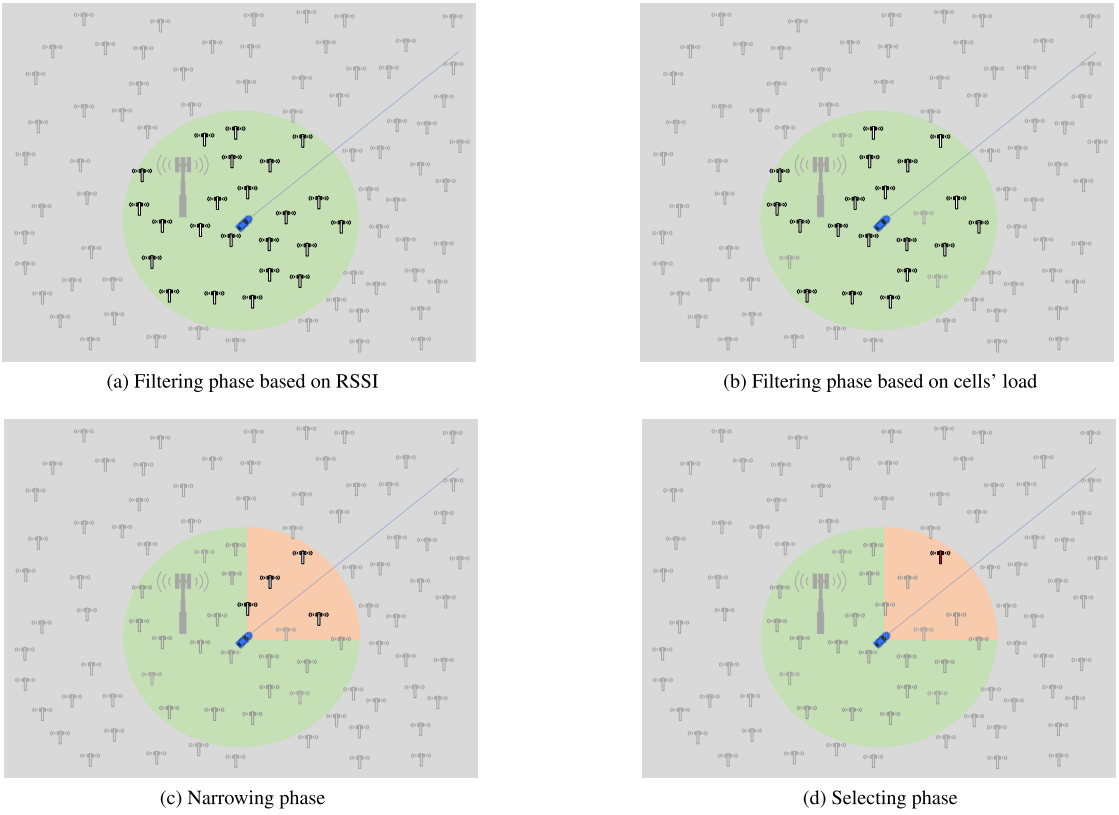

(a) Filtering phase based on RSSI

(b) Filtering phase based on cells' load

(c) Narrowing phase

(d) Selecting phase

FIGURE 2. Example of the proposed cell selection scheme.

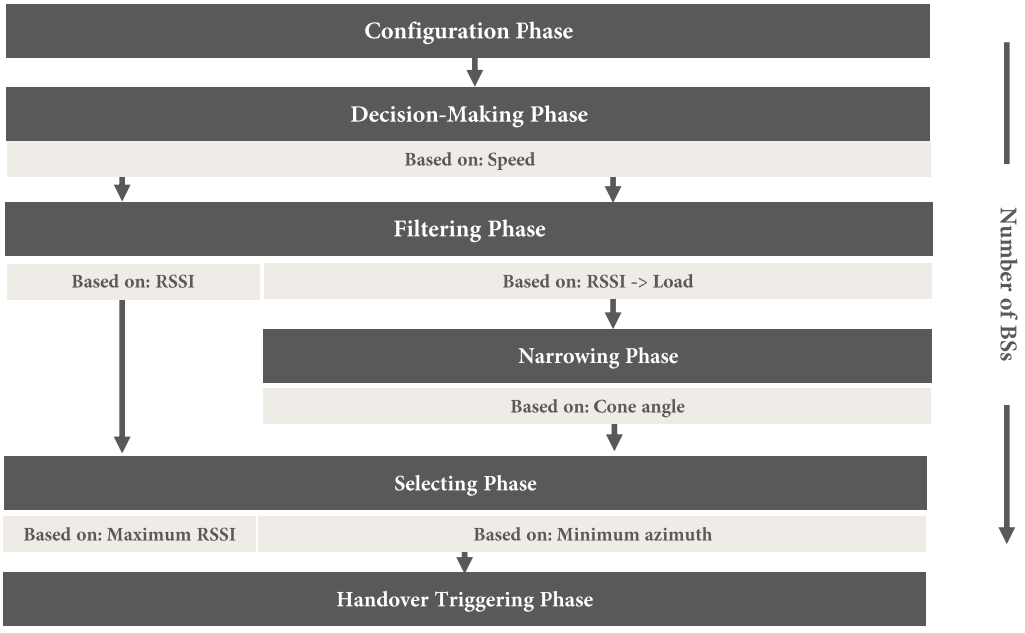

FIGURE 3. Phases of the proposed cell selection strategy.

1) Vehicle association constraint: A user vehicle can be associated with only one BS at a time, where a hard HO is applied. Therefore, we have

$$C1 : \sum_{j} a_{ij} = 1, \quad \forall\, v_i \in \mathcal{V}. \tag{9}$$

This constraint can be bypassed when a soft HO technique is applied to allow vehicles to perform make-before-break handovers.

2) Number of associated vehicles constraint: The number of vehicles associated with a BS b_j should not exceed the effective load of the BS, which is denoted

as L_j

$$C2: \sum_i a_{ij} = L_j, \quad \forall\, b_j \in \mathcal{B};\ 0 \le L_j \le N_V. \quad (10)$$

3) Total power constraint: The maximum transmission power limit of vehicle v_i, denoted as $p_{tx_{max}}$, from BS b_j should not be exceeded.

$$C3: \sum_i a_{ij} p_{tx_{ij}} \le p_{tx_{max}}, \quad \forall\, b_j \in \mathcal{B}. \quad (11)$$

4) QoS constraint: The minimum achievable data rate for each vehicle, denoted as R_{min}, should be maintained.

$$C4: \sum_j a_{ij} r_{ij} \ge R_{min}, \quad \forall\, v_i \in \mathcal{V}. \quad (12)$$

5) Cross-tier interference constraint: the summation of cross-tier interference should not exceed the maximum interference limit, denoted as I_{max}.

$$C5: \sum_i \sum_{k \in \mathcal{B}, k \ne j} a_{ij} p_{tx_{kj}} \zeta(d)_{kj} h_{kj} \leqslant I_{max}, \quad \forall\, b_j \in \mathcal{B}. \quad (13)$$

6) Service constraint: the dwell time in a cell (C/s) should exceed the HO latency, denoted by τ_i to avoid service interruption.

$$C6: C > \tau_i s, \quad \forall\, b_j \in \mathcal{B}\ \&\ v_i \in \mathcal{V} \quad (14)$$

IV. SYSTEM MODEL

A. DEPLOYMENT AND OPERATION MODEL

This study considers a mmWave-based ultra-dense network consisting of two tiers of BSs. Tier 1 includes traditional macro-cells, and tier 2 consists of high-density 5G small cells. Small BSs work in overlay with the macro BSs, where the macro BS tier operates at a carrier frequency of 2 GHz with a bandwidth of 10 MHz, while a carrier frequency of 28 GHz is used by the small BS tier with a bandwidth of 500 MHz. The available spectrum is shared among base stations based on a graph-coloring algorithm [58], which is described in section IV-D. Macro BS is assumed to be placed on a regular hexagonal grid. Small cells are distributed randomly within macro-cells, as shown in figure 4.

User vehicles are deployed randomly within the range of the network. Each vehicle has related information, such as the initial location, speed (km/h), and azimuth (degree). The vehicle association in the downlink of such a network is considered and the hard HO is assumed. The position of vehicles is updated every t_c milliseconds based on vehicle direction and speed. In this paper, network-initiated handover is considered, where a vehicle initiates the handover process, selects the target BS and informs the network, which decides whether the handover is performed or not.

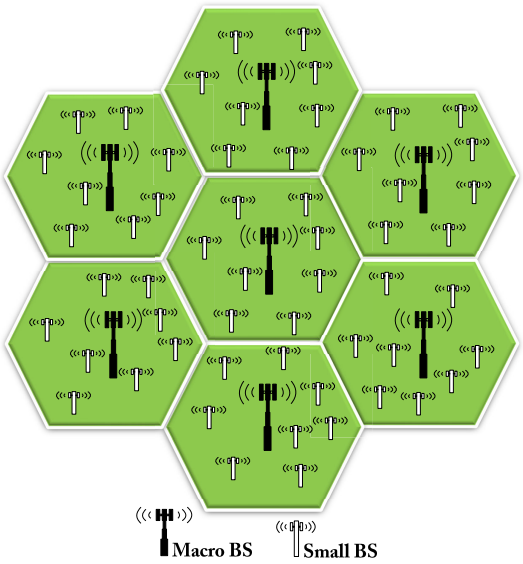

FIGURE 4. System model.

B. CHANNEL MODEL

In this study, 3GPP path loss models are used on the basis of 3GPP TR 38.901 version 16.1.0 in [59]. In an urban macro-cell (UMa) environment, the height of BSs is higher than that of the surrounding buildings. However, the height of BSs is shorter than that of the surrounding buildings in an urban microcell (UMi) environment. Table 2 shows that the path loss models that are used for macro and small tiers are 3GPP UMa and UMi, respectively. For the macro BS tier, the UMa-NLOS model is defined in equation (15).

$$PL_{UMa-NLOS} = max(PL_{UMa-NLOS}, PL'_{UMa-NLOS}) \quad (15)$$

TABLE 2. Simulation parameters.

Simulation Parameters	Values	
	Macro BS	Small BS
Number of BSs	7	600 /km^2
Carrier frequency (GHz)	2	28
System bandwidth (MHz)	10	500
Transmit power (dBm)	46	30
Path loss model (dB)	3GPP UMa Model	3GPP UMi Model
Standard deviation of shadow factor (dB)	6	4
Height (m)	25	10
Cell radius (m)	1400	200
Layout	Hexagonal grid	
Number of vehicles	4	
Vehicle speeds (km/h)	[20-120]	
Vehicle height (m)	1.8	
RSSI threshold (dBm)	-80	
Speed threshold (km/h)	80	
Load threshold (%)	90	
Cone angle (degree)	90	
Thermal noise density (dBm/Hz)	-174	
Shadowing	Log-normal	
Fast fading	Rayleigh fading	
Handover delay (ms)	50	
Simulation time (s)	180	

$$PL'_{UMa-NLOS} = 13.54 + 39.08\ log_{10}(d) + 20\ log_{10}(f_c) - 0.6(h_V - 1.5) \quad (16)$$

where f_c is the carrier frequency (GHz) and d is the distance between a macro BS and a vehicle in meters. The height of a vehicle in meters is denoted as h_V and it must satisfy 1.5 m $\leqslant h_V \leqslant$ 22.5 m condition.

For a small BS tier, the UMi-LOS (street canyon) model is represented in equation (17).

$$PL_{UMi-LOS} = \begin{cases} PL_1 & 10\ m \leqslant d \leqslant d'_{BP} \\ PL_2 & d'_{BP} \leqslant d \leqslant 5\ km \end{cases} \quad (17)$$

$$PL_1 = 32.4 + 21\ log_{10}(d) + 20\ log_{10}(f_c) \quad (18)$$

$$PL_2 = 32.4 + 40\ log_{10}(d) + 20\ log_{10}(f_c) - 9.5\ log_{10}((d'_{BP})^2 + (h_{BS} - h_V)^2) \quad (19)$$

where d'_{BP} is the breakpoint distance defined in equation (20). The height of the BS and the effective BS antenna height are denoted by h_{BS} and h'_{BS}, respectively. The effective height of the vehicle is represented by h'_V. The velocity of light in free space (c) equals 3 x 10^8 m/s.

$$d'_{BP} = 4\ h'_{BS}\ h'_V\ f_c/c \quad (20)$$

$$h'_{BS} = h_{BS} - h_E \quad (21)$$

$$h'_V = h_V - h_E \quad (22)$$

As shown in equation (23), the effective height, h_E, equals 1 m for UMi. For UMa, h_E equals 1 m with a probability of 1/(1+M) and it is selected from a discrete uniform distribution (12,15, . . . ,(h_V-1.5)) otherwise. Equation (24) shows the definition of M.

$$h_E = \begin{cases} 1\ m & for\ UMi \\ 1\ m & for\ UMa \\ with\ probability = (\frac{1}{1+M}) & \\ (12, 15, \ldots (h_V - 1.5))\ m & for\ UMa \\ with\ probability = (\frac{M}{1+M}) & \end{cases} \quad (23)$$

$$M = \begin{cases} 0 & h_V < 13\ m \\ (\frac{h_V - 13}{10})^{1.5}\ g & 13m \leqslant h_V \leqslant 23\ m \end{cases} \quad (24)$$

$$g = \begin{cases} 0 & d \leqslant 18\ m \\ (\frac{5}{4})(\frac{d}{100})^3\ exp(\frac{-d}{150}) & 18m < d \end{cases} \quad (25)$$

Equation (26) gives the standard deviations of shadow fading, σ_{SF}, of UMi and UMa. Shadowing is assumed to be log-normal. The Rayleigh-fading channel should exist between a vehicle and the connected BS. It is an exponentially distributed random variable with a unit mean.

$$\sigma_{SF} = \begin{cases} 4\ dB & for\ UMi \\ 6\ dB & for\ UMa \end{cases} \quad (26)$$

C. NUMBER OF HANDOVERS

Handover (HO) or handoff is defined as the process of transferring a connection from a current serving BS to another in the network [60], which is a critical process to address in wireless cellular networks due to the mobility of the UE [61]. Figure 5 presents the principal symbols used to prove the HO laws used in this section. R is the radius of a cell, whether it is a macro -cell or a small cell. The entering angle to move into a cell and the exiting angle to move out of the cell are denoted by θ_i and θ_o, respectively. Vehicle speed is represented by s. T is the dwell time within the cell. A chord of a circle is a line of which both endpoints lie on the boundary of the circle [62]. The dwell distance is denoted by a random chord (C) of the coverage circle that passes through points P_i and P_o. The angle subtended by the chord is represented by Θ. The symbol A is the apothem of the circle, which is a line segment from the BS to the center point of the circle chord. The sagitta of the circle is denoted by S, which is a line segment from the chord's center point to the midpoint of the arc subtended by the chord [63], [64].

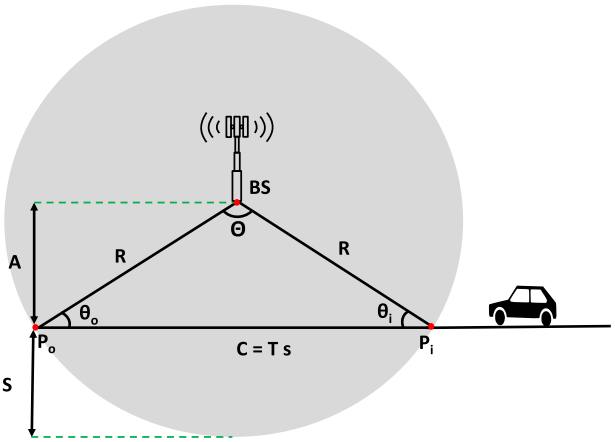

FIGURE 5. Illustration of the principal symbols used to prove the probabilities of HO failure and unnecessary HO.

Handover failure (HOF) occurs if a handover process is initiated but not completed [65]. In other words, it happens when the dwell time inside a cell is shorter than HO latency (τ_i) [66].

Lemma 1: Let HO latency to move into a cell be denoted by τ_i and the time threshold of HOF be denoted by T_1; then,

$$P_{HOF} = \begin{cases} \frac{2}{\pi}[\sin^{-1}(\frac{s\tau_i}{2R}) - \sin^{-1}(\frac{sT_1}{2R})] & 0 \leqslant T_1 \leqslant \tau_i \\ 0 & \tau_i < T_1 \end{cases} \quad (27)$$

and

$$T_1 = \frac{2R}{s} sin(sin^{-1}(\frac{s\tau_i}{2R}) - \frac{2}{\pi}P_{HOF}); \quad 0 \leqslant P_{HOF} \leqslant 1 \quad (28)$$

Proof: Please see Appendix.

Unnecessary handover (UHO), or false handover, is defined as the meaningless operation of switching a vehicle

connection from one BS to another [67]. It occurs when the total dwell time of a vehicle within a cell is smaller than the total HO latencies for moving in and out of the cell [66].

Lemma 2: Let HO latencies to move into a cell and to move out of the cell be τ_i and τ_o and the time threshold of UHO be denoted by T_2; then,

$$P_{UHO} = \begin{cases} \frac{2}{\pi}[\sin^{-1}(\frac{s(\tau_i+\tau_o)}{2R}) \\ \quad -\sin^{-1}(\frac{sT_2}{2R})] & 0 \leqslant T_2 \leqslant (\tau_i+\tau_o) \\ 0 & (\tau_i+\tau_o) < T_2 \end{cases} \quad (29)$$

and

$$T_2 = \frac{2R}{s}\sin(\sin^{-1}(\frac{s(\tau_i+\tau_o)}{2R}) - \frac{2}{\pi}P_{UHO}); \quad 0 \leqslant P_{UHO} \leqslant 1 \quad (30)$$

Proof: Please see Appendix.

Equations (28) and (30) are derived from equations (27) and (29) for specific values of P_{HOF} and P_{UHO}. In this study, the target P_{HOF} and P_{UHO} are assumed to be 2% and 4%, respectively.

The number of HOF, N_{HOF}, is calculated using equation (31). Equation (32) calculates the number of UHO, N_{UHO}, where N_{HO} is the total number of handovers.

$$N_{HOF} = P_{HOF} \times N_{HO} \quad (31)$$

$$N_{UHO} = P_{UHO} \times N_{HO} \quad (32)$$

D. DATA RATES AND SPECTRAL EFFICIENCY

Small cells enabling technology aims to provide high capacity and spectral efficiency with low deployment cost [68], [69]. The achievable downlink data rate is based on the signal-to-interference-plus-noise ratio (SINR) and channel resource allocation. Equation (33) represents SINR formula at a vehicle v_i that is associated with BS $b_j \in \mathcal{B}$.

$$\gamma_{ij} = \frac{p_{tx_j}\zeta_{ij}(d)h_{ij}}{\sum_{k\neq j}(p_{tx_k}\zeta_{ik}(d)h_{ik}) + \delta^2}, \quad \forall v_i \in \mathcal{V} \text{ and } \forall\, b_j \in \mathcal{B}. \quad (33)$$

where p_{tx} is the transmission power of base station b_j and $\zeta(d)$ is the path loss function associated with distance d. The channel gain is denoted as h, which includes shadowing and Rayleigh fading, as described in section IV-B. The interference issue between cells is managed based on a graph-coloring algorithm [58]. The reason behind selecting this method is that it is an efficient way to manage interference problems in a random topology network, such as UDN [58], [70]. The interference graph is modeled as $G = (N, L)$ where N signifies nodes that represent BSs and L are links between two adjacent BSs. The available frequency resources are modeled as colors, where each node must have a color, with the constraint that two adjacent nodes should use different frequency resources and the number of colors should be as few as possible. Therefore, interference can be avoided by assigning different colors (resources) to adjacent BSs.

δ^2 is the additive white Gaussian noise (AWGN) power, which can be calculated as shown in equation (34), where N_0 and BW are noise power spectral density and subchannel bandwidth, respectively.

$$\delta^2 = N_o BW \quad (34)$$

Based on Shannon's formula, the achievable downlink data rate when the vehicle v_i associated with base station b_j is given by equation (35). Spectral efficiency (SE) of vehicle v_i served by BS b_j, is given in equation (36).

$$r_{ij} = BW \ \ log_2(1+\gamma_{ij}) \quad (35)$$

$$\eta_{ij} = \frac{r_{ij}}{BW} \quad (36)$$

V. SIMULATION RESULTS AND DISCUSSION

In this section, the proposed adaptive cell selection scheme is evaluated using a MATLAB simulator. The performance metrics for this study are the average dwell time, average number of HOs, average number of HOFs, average number of UHOs, and average achievable downlink data rates and spectral efficiency per vehicle. The performance evaluation was studied from two perspectives, which are vehicle speeds (section V-A) and the small BSs density (section V-B). Furthermore, a comparison has been performed among the proposed ADA-CS scheme, the traditional cell selection scheme, and four methods proposed by Kapoor *et al.* [34].

A two-tier HUDN with seven macro-cells and high-density small cells that are uniformly overlaid on the edge is studied. The maximum transmission power of macro and small BSs is set to 46 and 30 dBm, respectively. The thermal noise density is -74 dBm/Hz. The radius of the macro-cells and small cells is 1400 m and 200 m, respectively. Table 2 shows the simulation parameters.

A. RESULTS FROM VEHICLE SPEEDS PERSPECTIVE

This section focuses on evaluating the HUDN performance in view of vehicle speeds, where speeds from 20 to 120 km/h are considered. Figures 6 and 7 show the relationship between the average dwell time and average number of HOs versus vehicle speeds. As shown in the figures, as vehicle speed increases, the dwell time decreases and the number of HOs increases. The proposed ADA-CS protocol aims to select cells that have the longest dwell time. However, it defines a certain speed threshold (80 km/h in this example). Thus, when the speed threshold is exceeded, the vehicle's association is switched to the nearest macro BS to avoid the ping-pong effect. The traditional RSSI-based method is the worst in terms of the dwell time and, thus, the number of HOs. The reason for this is that it chooses the closest BS which has the strongest RSSI, regardless of the direction of a vehicle. Therefore, ADA-CS outperforms it in terms of average number of HOs by 42.39% when the $\hat{S}$ is not exceeded. The MD scheme is the second worst protocol because it selects the BS that has the strongest RSSI in the vehicle's direction. Thus, our proposed protocol achieves superiority by 36.53%.

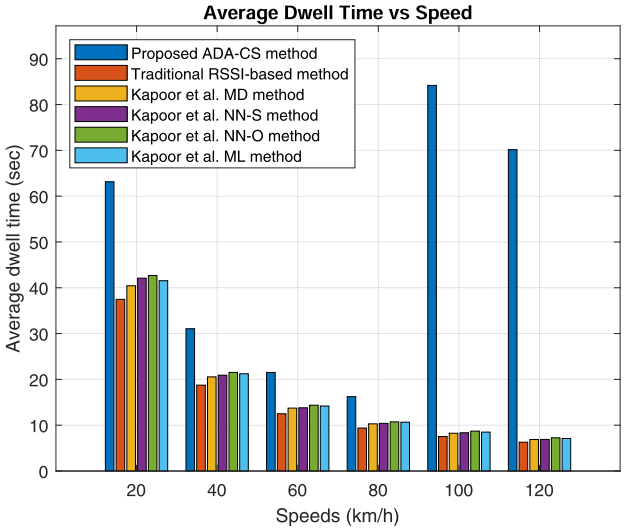

FIGURE 6. Average dwell time vs speed.

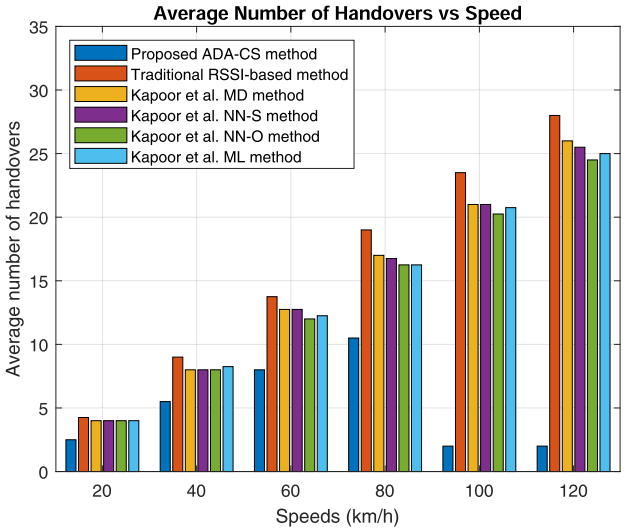

FIGURE 7. Average number of handovers vs speed.

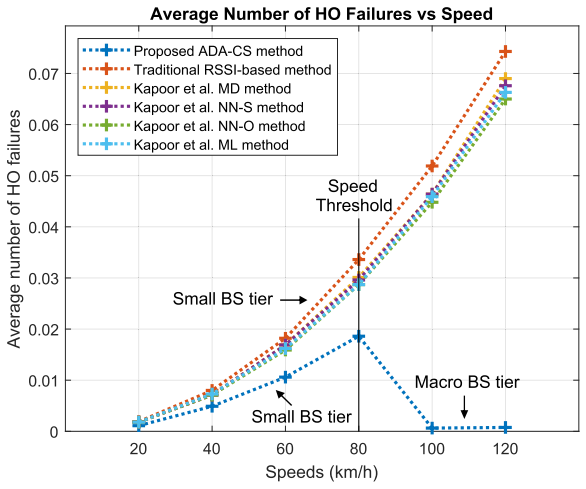

(a) Average number of handover failures vs speed.

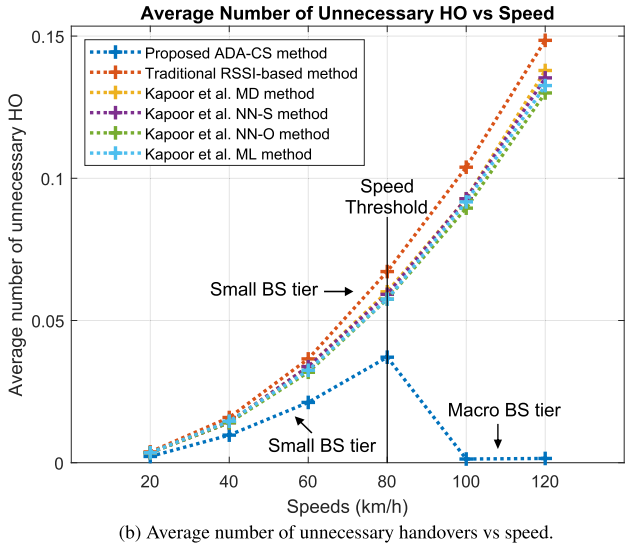

(b) Average number of unnecessary handovers vs speed.

FIGURE 8. Average number of handover failures and unnecessary handovers. The ADA-CS algorithm switches from the small BS tier to the macro BS tier when a speed threshold (80 km/h in this example) is exceeded, to avoid increasing the average numbers of HOFs and UHOs.

The NN-S scheme limits its choice to a BS that has the maximum azimuth angle from the k-nearest neighbor list in the range $[0,\pi/2]$. Our ADA-CS outperforms the NN-S scheme in terms of the average number of HOs by 36.14%. For the ML method, the cell selection depends on the load value, which is a variable value based on the number of associated vehicles. Relying on load value to choose a cell without considering the dwell time is not sufficient. Thus, the proposed ADA-CS surpasses it by 34.97%. NN-O is the best scheme among Kapoor *et al.*'s methods in terms of the average dwell time and average number of HOs because it chooses the BS from the k-nearest neighbor list in the range $[\pi/2,\pi]$ that has the minimum azimuth angle. Therefore, the entry point will be before the center of the cell and, thus, the dwell time will be longer than the rest of Kapoor *et al.*'s schemes. However, NN-O still gives priority to small BSs that have the highest received signal, so our scheme surpasses it by 34.16%. With vehicles traveling at a speed higher than $\hat{S}$, additional improvements are achieved by ADA-CS due to the adaptation property that makes the vehicles associate with the macro BS tier. These improvements in the length of dwell time are estimated at up to 30.9% compared with the other protocols. Figure 8 shows the effect of vehicle speed on the average number of HOFs (Figure 8a) and the average number of UHOs (Figure 8b). The proposed ADA-CS method is superior to the traditional method for the average number of HOFs and UHOs by 42.95% and 43.11%, respectively. The reason is that the proposed protocol chooses a BS that a vehicle can stay associated with for the longest possible time. Kapoor *et al.*'s schemes give high priority to the nearby BSs that have the strongest RSSI, without regard to the dwell time and the speed

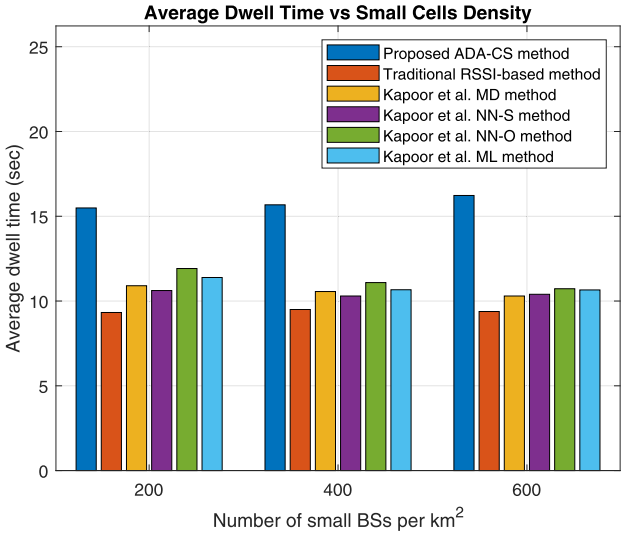

FIGURE 9. Average dwell time vs small cell density.

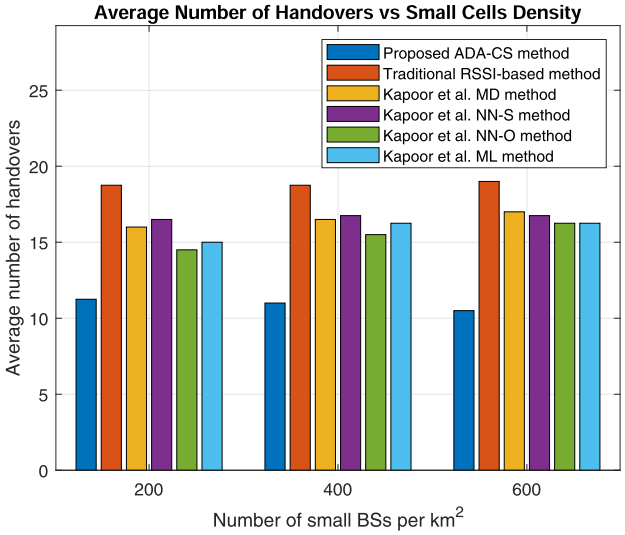

FIGURE 10. Average number of handovers vs small cell density.

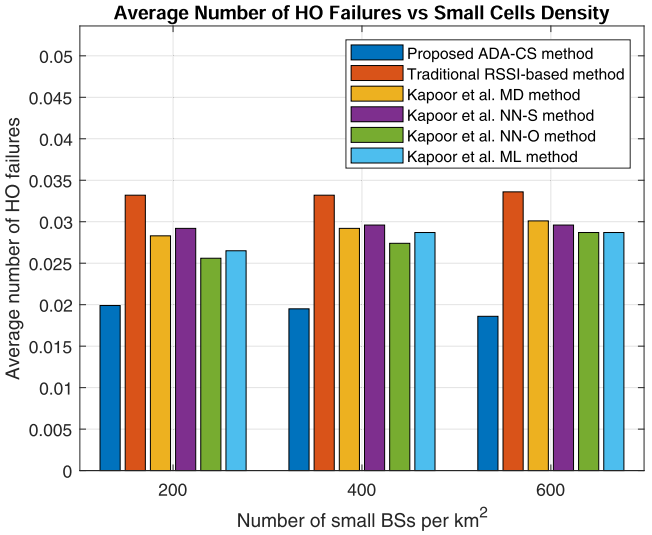

(a) Average number of handover failures vs small cell density.

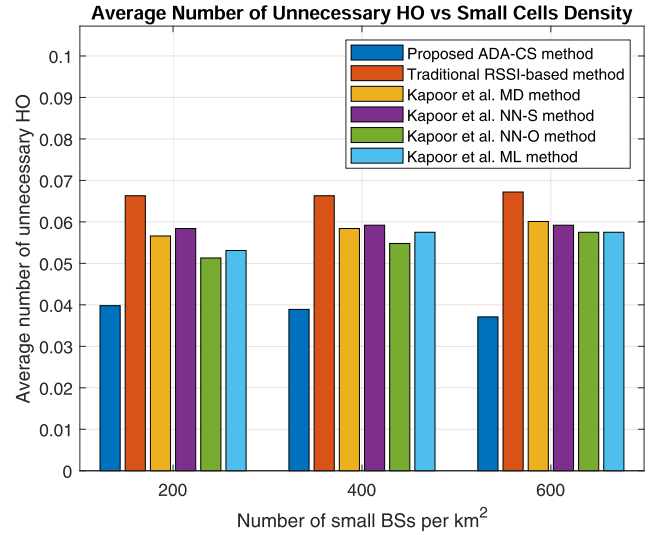

(b) Average number of unnecessary handovers vs small cell density.

FIGURE 11. Average number of and handover failures and unnecessary handovers.

of the vehicle. Therefore, the ADA-CS scheme outperformed them in terms of HOFs and UHOs by up to 37.3% and 37.04% with vehicles at speeds lower than $\hat{S}$. The ADA-CS algorithm avoids increasing the average numbers of HOFs and UHOs when speed increases by setting a speed threshold. Exceeding $\hat{S}$ leads to an association with the nearest macro BS instead of small BS to maintain an acceptable network performance level. Thus, ADA-CS achieves additional enhancement with vehicles at speeds greater than $\hat{S}$ by up to 43.17% and 43.3% in terms of HOFs and UHOs compared with the other cell selection strategies.

B. RESULTS FROM NETWORK DENSITY PERSPECTIVE

Future 5G cellular networks are expected to be dense because of the deployment of numerous small cells [71]. In this section, we have studied the impact of small cell density on the performance of the HUDN. In this scenario, the speed of a vehicle is assumed to be 80 km/h and the numbers of considered small BSs are 200, 400, and 600 small BSs/ km^2.

Figures 9 and 10 show the relationship between the density of small cells versus the average dwell time and the average number of HOs. On the basis of the proposed ADA-CS scheme, when the small cell density increases, there are more small BSs to choose from and thus the cell with the longest dwell time is selected. Increasing the density resulted in improvement in average dwell time and number of HOs by 2.35% and 3.38%. For traditional and Kapoor *et al.*'s protocols, increasing density means finding closer cells. When a small BS is not located in the vehicle's direction, making the small BS closer to the vehicle means increasing the dwell time. On the other hand, making the small BSs closer that

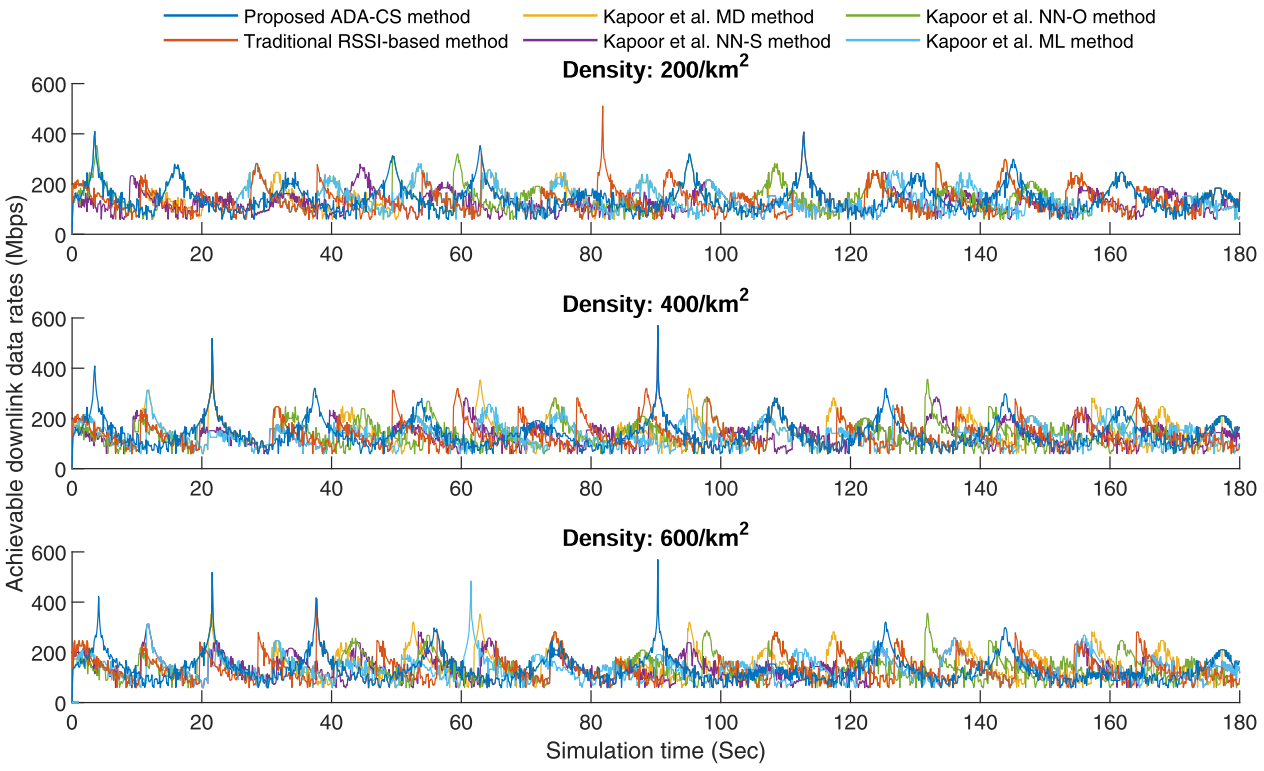

(a) Achievable downlink data rates.

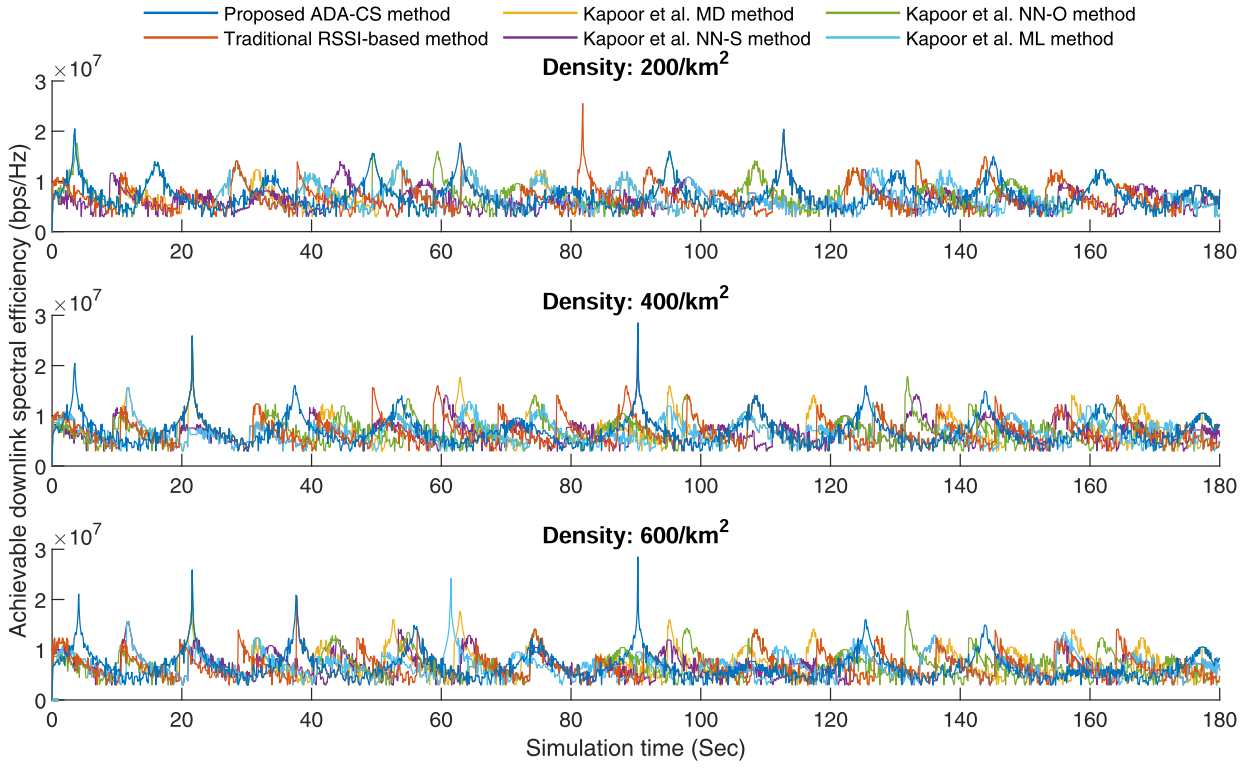

(b) Achievable downlink spectral efficiency.

FIGURE 12. Achievable downlink data rates and spectral efficiency per vehicle.

TABLE 3. List of abbreviations.

Abbreviation	Meaning
3GPP	Third-Generation Mobile Partnership Project
5G	Fifth-Generation
AWGN	Additive White Gaussian Noise
BBU	Baseband Unit
BS	Base Station
H-CRANs	Heterogeneous Cloud Radio Access Networks
HetNets	Heterogeneous Networks
HOF	Handover Failures
HUDNs	Heterogeneous Ultra-Dense Networks
IDs	Identifications
IoT	Internet of Things
KNN	K-Nearest Neighbor
LP	Linear Programming
LTE	Long Term Evolution
MAB	Multi-Armed Bandit
MD	Minimum Distance
MIMO	Multiple-Input Multiple-Output
mMIMO	massive MIMO
mmWave	millimeter Wave
NN-S	Next Neighbor on the Same street
OAA	Outer Approximation Approach
RANs	Radio Access Networks
RNN	Recurrent Neural Network
RRHs	Remote Radio Heads
RSSI	Received Signal Strength Indicator
SDN	Software- Defined Network
SINR	Signal-to-Interference-plus-Noise Ratio
SVM	Support Vector Machine
UE	User Equipment
UHO	Unnecessary Handovers
UMa	Urban Macro cell
Umi	Urban Micro cell
WCS	Worst Connection Swapping
XGBoost	eXtreme Gradient Boosting

are located in the vehicle's direction leads to a reduction in the dwell time. Therefore, the average number of HOs of the traditional method is increased by 0.66%. For Kapoor *et al.*'s schemes, the increase in the average number of HOs is up to 5.76%.

Figures 11a and 11b shows the impact of small cell density on the average number of HOFs and UHOs. The simulation results show that the proposed ADA-CS improves the average number of HOFs and UHOs by 3.42%. On the other hand, using the traditional cell selection method, the mean number of HOFs and UHOs increased by up to 0.67%. The average number of HOFs and UHOs deteriorated with Kapoor *et al.*'s methods by up to 5.55%.

Figure 12 shows the achievable downlink data rate (figure 12a) and spectral efficiency (figure 12b) of a vehicle during the simulation time with different small BSs density. As shown in the figure, we found that the proposed ADA-CS protocol selects the small cells in the vehicle's direction that have the longest dwell time. Therefore, a vehicle associates with a small cell when the vehicle is located at the edge of the cell and, whenever the vehicle moves forward, the achievable data rate increases. The data rate value reaches its peak when the vehicle is in the middle of the cell so that it is close to the small BS. Then, the data rate will decrease until the RSSI value is lower than the predefined RSSI threshold. In this way, the ADA-CS scheme guarantees a high average downlink data rate compared with the other methods. The traditional RSSI-based method selects the nearest small BS, whether it is located in the vehicle's direction or not. Vehicle movement leads to a decrease in the achievable data rates until $\hat{R}$ reached. Therefore, the average downlink data rate is less than under the ADA-CS scheme by 3.98%. Kapoor *et al.*'s schemes select small BSs in the vehicle's direction but they give high priority to the nearest small BSs. Thus, vehicle movement leads to a data-rate reduction and reaching the peak ADA-CS data-rate value is not always guaranteed. Consequently, our protocol outperforms Kapoor *et al.*'s methods by an average of 2.79%. As the spectral efficiency is the achievable data rate divided by occupied bandwidth, the ADA-CS algorithm is superior to other cell selection strategies for the reasons given here.

VI. CONCLUSION AND FUTURE WORK

Recently, the cell selection issue in 5G networks has attracted researchers' attention because the conventional RSSI-based method might no longer apply to the current generation of cellular networks. In this study, the problem of cell selection on the downlink of an HUDN is studied where single connectivity is enabled. An adaptive cell selection strategy is proposed that can adapt to various characteristics of vehicle movements and HUDN environments. To select an associated BS, the proposed algorithm passes through six phases. The simulation results prove that the proposed scheme achieves improvements over the traditional, MD, NN-S, NN-O, and ML cell selection schemes. In terms of the average number of HOs, it achieves superiority with low- and medium-speed vehicles by 42.39% compared with the traditional method and up to 36.53% in comparison to Kapoor *et al.*'s schemes. For high-speed vehicles, the adaptation property of the ADA-CS scheme allows it to achieve additional reduction of the average number of HOs by up to 29.96% compared with the other methods. ADA-CS can select the best BS, with the longest dwell time, to avoid the ping-pong effect. Furthermore, it achieves superiority regarding the average number of HOFs and average number of UHOs. Regarding the achievable downlink data rates and spectral efficiency, the ADA-CS strategy is superior to the traditional and Kapoor *et al.*'s schemes by 3.98% and 2.79%, respectively. For future work, studies will be performed to assess the effect of changing the values of the proposed protocol thresholds; namely, speed, load, and RSSI. Furthermore, a comparison of the impact of cone angle values on network performance can be applied. Additional performance metrics can be applied, such as the vehicle's power consumption, energy efficiency, and delay. Energy can be saved explicitly by introducing two power-operating modes for small base station, i.e., awake and sleeping modes that operate according to the traffic loads. The proposed cell selection strategy can be enhanced to accomplish the cell selection process based on machine learning

techniques, such as eXtreme Gradient Boosting (XGBoost), support vector machine (SVM), KNN, and RNN.

APPENDIX
PROOF OF LEMMA 1 AND 2

Proof: When a vehicle enters and exits a cell, it intersects the coverage circle at two points (P_i and P_o) forming a random chord (C), (Figure 5). The length of any chord can be calculated by knowing the values of the radius (R) length and the measurement of the angle subtended by the chord (Θ). To prove lemma 1, we first derive the length of C, which can be denoted as

$$\begin{aligned} \sin(\Theta/2) &= \frac{0.5C}{R} \\ C &= 2R\sin(\Theta/2) \end{aligned} \tag{37}$$

Using equation (37), the formula of the angle Θ can be given as

$$\Theta = 2\ \sin^{-1}\ (\frac{C}{2R}) \tag{38}$$

If Θ is uniformly distributed between $[0, \pi]$ then,

$$\begin{aligned} Pr[0 \le \Theta \le \pi] &= g(\Theta) \\ &= \frac{1}{\pi} \end{aligned} \tag{39}$$

The probability density function (PDF) of the chord C is given by

$$f(C) = g(\Theta).\frac{d\Theta}{dC} \tag{40}$$

$$\begin{aligned} \frac{d\Theta}{dC} &= \frac{d}{dC}[2\ \sin^{-1}(\frac{C}{2R})] \\ &= \frac{2}{\sqrt{1-(\frac{C}{2R})^2}}.\frac{d}{dC}[\frac{C}{2R}] \\ &= \frac{1}{R\sqrt{\frac{4R^2-C^2}{4R^2}}} \\ &= \frac{2}{\sqrt{4R^2-C^2}} \end{aligned} \tag{41}$$

By substituting equations (39) and (41) into equation (40), we obtain

$$f(C) = \frac{2}{\pi\sqrt{4R^2-C^2}} \tag{42}$$

Next, we focus on calculating P_{HOF}, which is defined as the probability that the dwell time of the vehicle in a cell falls within a range between T_1 and τ_i. On the basis of integration by substitution where $u = \frac{iC}{2R}$ and $\frac{du}{dC} = \frac{i}{2R}$, we have

$$\begin{aligned} P_{HOF} &= Pr\ [T_1 \le T \le \tau_i] \\ &= Pr\ [sT_1 \le C \le s\tau_i] \\ &= \int_{sT_1}^{s\tau_i} f(C)\, dC \\ &= \int_{sT_1}^{s\tau_i} \frac{2}{\pi\sqrt{4R^2-C^2}} dC \\ &= \int_{sT_1}^{s\tau_i} -\frac{4iR}{\pi\sqrt{4R^2u^2+4R^2}} du \\ &= -\frac{2i}{\pi}\int_{sT_1}^{s\tau_i} \frac{1}{\sqrt{u^2+1}} du \\ &= -\frac{2i}{\pi}\ln(\sqrt{u^2+1}+u)\Big|_{sT_1}^{s\tau_i} \\ &= -\frac{2i}{\pi}\ln(|\sqrt{1-\frac{C^2}{4R^2}}+\frac{iC}{2R}|)\Big|_{sT_1}^{s\tau_i} \\ &= -\frac{2i}{\pi}\ln(|R\sqrt{4R^2-C^2}+i|R|C|)\Big|_{sT_1}^{s\tau_i} \\ &= [\frac{2}{\pi}\sin^{-1}(\frac{C}{2R})]\Big|_{sT_1}^{s\tau_i} \\ &= \frac{2}{\pi}[\sin^{-1}(\frac{s\tau_i}{2R}) - \sin^{-1}(\frac{sT_1}{2R})] \end{aligned} \tag{43}$$

According to equation (43), the formula of the time threshold of HOFs (T_1) is given by

$$\begin{aligned} \frac{2}{\pi}\sin^{-1}(\frac{sT_1}{2R}) &= \frac{2}{\pi}\sin^{-1}(\frac{s\tau_i}{2R}) - P_{HOF} \\ T_1 &= \frac{2R}{s}\sin\ [\sin^{-1}(\frac{s\tau_i}{2R}) - \frac{\pi}{2}P_{HOF}] \end{aligned} \tag{44}$$

The proof of lemma 2 can be driven similarly based on the definition of P_{UHO}. The probability of UHOs means that the dwell time of the vehicle in a cell falls within a range between T_2 and $(\tau_i + \tau_o)$.

$$\begin{aligned} P_{UHO} &= Pr\ [T_2 \le T \le (\tau_i+\tau_o)] \\ &= Pr\ [sT_2 \le C \le s(\tau_i+\tau_o)] \\ &= \int_{sT_2}^{s(\tau_i+\tau_o)} f(C)\, dC \\ &= \int_{sT_2}^{s(\tau_i+\tau_o)} \frac{2}{\pi\sqrt{4R^2-C^2}} dC \\ &= \int_{sT_2}^{s(\tau_i+\tau_o)} -\frac{4iR}{\pi\sqrt{4R^2u^2+4R^2}} du \\ &= -\frac{2i}{\pi}\int_{sT_2}^{s(\tau_i+\tau_o)} \frac{1}{\sqrt{u^2+1}} du \\ &= -\frac{2i}{\pi}\ln(\sqrt{u^2+1}+u)\Big|_{sT_2}^{s(\tau_i+\tau_o)} \\ &= -\frac{2i}{\pi}\ln(|\sqrt{1-\frac{C^2}{4R^2}}+\frac{iC}{2R}|)\Big|_{sT_2}^{s(\tau_i+\tau_o)} \\ &= -\frac{2i}{\pi}\ln(|R\sqrt{4R^2-C^2}+i|R|C|)\Big|_{sT_2}^{s(\tau_i+\tau_o)} \\ &= [\frac{2}{\pi}\sin^{-1}(\frac{C}{2R})]\Big|_{sT_2}^{s(\tau_i+\tau_o)} \\ &= \frac{2}{\pi}[\sin^{-1}(\frac{s(\tau_i+\tau_o)}{2R}) - \sin^{-1}(\frac{sT_2}{2R})] \end{aligned} \tag{45}$$

On the basis of equation (45), the formula of the time threshold of UHOs (T_2) is given by

$$\begin{aligned} \frac{2}{\pi}\sin^{-1}(\frac{sT_2}{2R}) &= \frac{2}{\pi}\sin^{-1}(\frac{s(\tau_i+\tau_o)}{2R}) - P_{UHO} \\ T_2 &= \frac{2R}{s}\sin\ [\sin^{-1}(\frac{s(\tau_i+\tau_o)}{2R}) - \frac{\pi}{2}P_{UHO}] \end{aligned} \tag{46}$$

ACKNOWLEDGMENT

The authors thank the Deanship of Scientific Research and RSSU at King Saud University for their technical support.

CONFLICTS OF INTEREST

The authors declare no conflict of interest.

REFERENCES

[1] Y. Lei, G. Zhu, C. Shen, Y. Xu, and X. Zhang, "Delay-aware user association and power control for 5G heterogeneous network," *Mobile Netw. Appl.*, vol. 24, no. 2, pp. 491–503, Apr. 2019.

[2] I. Alablani and M. Alenazi, "Performance evaluation of sensor deployment strategies in WSNs towards IoT," in *Proc. IEEE/ACS 16th Int. Conf. Comput. Syst. Appl. (AICCSA)*, Nov. 2019, pp. 1–8.

[3] Y. M. Waheidi, M. Jubran, and M. Hussein, "User driven multiclass cell association in 5G HetNets for mobile & IoT devices," *IEEE Access*, vol. 7, pp. 82991–83000, 2019.

[4] I. Alablani and M. Alenazi, "EDTD-SC: An IoT sensor deployment strategy for smart cities," *Sensors*, vol. 20, no. 24, p. 7191, Dec. 2020.

[5] S. L. Aljohani and M. J. F. Alenazi, "MPResiSDN: Multipath resilient routing scheme for SDN-enabled smart cities networks," *Appl. Sci.*, vol. 11, no. 4, p. 1900, Feb. 2021.

[6] B. U. Kazi and G. A. Wainer, "Next generation wireless cellular networks: Ultra-dense multi-tier and multi-cell cooperation perspective," *Wireless Netw.*, vol. 25, no. 4, pp. 2041–2064, May 2019.

[7] D. Liu, L. Wang, Y. Chen, M. Elkashlan, K.-K. Wong, R. Schober, and L. Hanzo, "User association in 5G networks: A survey and an outlook," *IEEE Commun. Surveys Tuts.*, vol. 18, no. 2, pp. 1018–1044, 2nd Quart., 2016.

[8] Z. Bojkovic and D. Milovanovic, "A technology vision of the fifth generation (5G) wireless mobile networks," in *Proc. Int. Conf. Emerg. Trends Electr., Electron. Commun. Eng.* Cham, Switzerland: Springer, 2016, pp. 25–43.

[9] J. Zhao, Y. Liu, Y. Gong, C. Wang, and L. Fan, "A dual-link soft handover scheme for C/U plane split network in high-speed railway," *IEEE Access*, vol. 6, pp. 12473–12482, 2018.

[10] Nidhi and A. Mihovska, "Small cell deployment challenges in ultradense networks: Architecture and resource management," in *Proc. 12th Int. Symp. Commun. Syst., Netw. Digit. Signal Process. (CSNDSP)*, Jul. 2020, pp. 1–6.

[11] W.-S. Kim, G. J. Van Lieshout, S.-H. Kim, and S.-B. Kim, "Method and apparatus for reporting buffer state by user equipment in communication system," U.S. Patent 10 708 940, Jul. 7, 2020.

[12] A. Gotsis, S. Stefanatos, and A. Alexiou, "UltraDense networks: The new wireless frontier for enabling 5G access," *IEEE Veh. Technol. Mag.*, vol. 11, no. 2, pp. 71–78, Jun. 2016.

[13] L. Xu, Y. Mao, S. Leng, G. Qiao, and Q. Zhao, "Energy-efficient resource allocation strategy in ultra dense small-cell networks: A Stackelberg game approach," in *Proc. IEEE Int. Conf. Commun. (ICC)*, May 2017, pp. 1–6.

[14] M. Kamel, W. Hamouda, and A. Youssef, "Ultra-dense networks: A survey," *IEEE Commun. Surveys Tuts.*, vol. 18, no. 4, pp. 2522–2545, May 2016.

[15] *Ultra Dense Network (UDN) White Paper*, Nokia Solutions Neworks Oy, Espoo, Finland, 2016.

[16] D. G. González, E. Mutafungwa, B. Haile, J. Hämäläinen, and H. Poveda, "A planning and optimization framework for ultra dense cellular deployments," *Mobile Inf. Syst.*, vol. 2017, pp. 1–17, Mar. 2017.

[17] Y. Wei and S.-H. Hwang, "Optimization of cell size in ultra-dense networks with multiattribute user types and different frequency bands," *Wireless Commun. Mobile Comput.*, vol. 2018, pp. 1–10, Oct. 2018.

[18] A. Mesodiakaki, E. Zola, and A. Kassler, "User association in 5G heterogeneous networks with mesh millimeter wave backhaul links," in *Proc. IEEE 18th Int. Symp. World Wireless, Mobile Multimedia Netw. (WoWMoM)*, Jun. 2017, pp. 1–6.

[19] H. Zhang, S. Huang, C. Jiang, K. Long, V. C. M. Leung, and H. V. Poor, "Energy efficient user association and power allocation in millimeter-wave-based ultra dense networks with energy harvesting base stations," *IEEE J. Sel. Areas Commun.*, vol. 35, no. 9, pp. 1936–1947, Sep. 2017.

[20] Z. Qin, X. Yue, Y. Liu, Z. Ding, and A. Nallanathan, "User association and resource allocation in unified NOMA enabled heterogeneous ultra dense networks," *IEEE Commun. Mag.*, vol. 56, no. 6, pp. 86–92, Jun. 2018.

[21] X. Wang, Y. Xu, J. Wang, and S. Fu, "Joint user association and power allocation in heterogeneous NOMA networks with imperfect CSI," *IEEE Access*, vol. 8, pp. 47607–47618, 2020.

[22] M. Tayyab, G. P. Koudouridis, X. Gelabert, and R. Jäntti, "Uplink reference signals for energy-efficient handover," *IEEE Access*, vol. 8, pp. 163060–163076, 2020.

[23] S. Goyal, M. Mezzavilla, S. Rangan, S. Panwar, and M. Zorzi, "User association in 5G mmWave networks," in *Proc. IEEE Wireless Commun. Netw. Conf. (WCNC)*, Mar. 2017, pp. 1–6.

[24] A. Kishida, Y. Morihiro, T. Asai, and Y. Okumura, "Cell selection scheme for handover reduction based on moving direction and velocity of UEs for 5G multi-layered radio access networks," in *Proc. Int. Conf. Inf. Netw. (ICOIN)*, Jan. 2018, pp. 362–367.

[25] S. Kumar, "A survey on handover in LTE heterogeneous networks," in *Proc. Int. Conf. IoT Inclusive Life (ICIIL)*. Chandigarh, India: Springer, 2020, pp. 111–125.

[26] T. M. Duong and S. Kwon, "Vertical handover analysis for randomly deployed small cells in heterogeneous networks," *IEEE Trans. Wireless Commun.*, vol. 19, no. 4, pp. 2282–2292, Apr. 2020.

[27] Y. Yang, J. Xu, G. Shi, and C.-X. Wang, *5G Wireless Systems*. New York, NY, USA: Springer, 2018.

[28] Z. Han, T. Lei, Z. Lu, X. Wen, W. Zheng, and L. Guo, "Artificial intelligence-based handoff management for dense WLANs: A deep reinforcement learning approach," *IEEE Access*, vol. 7, pp. 31688–31701, 2019.

[29] R. Abdullah and Z. Zukarnain, "Enhanced handover decision algorithm in heterogeneous wireless network," *Sensors*, vol. 17, no. 7, p. 1626, Jul. 2017.

[30] N. Hassan and X. Fernando, "An optimum user association algorithm in heterogeneous 5G networks using standard deviation of the load," *Electronics*, vol. 9, no. 9, p. 1495, Sep. 2020.

[31] M. N. Sial and J. Ahmed, "A realistic uplink–downlink coupled and decoupled user association technique for K-tier 5G HetNets," *Arabian J. Sci. Eng.*, vol. 44, no. 3, pp. 2185–2204, Mar. 2019.

[32] G. Kosztolanyi-Ivan, C. Koren, and A. Borsos, "Recognition of road types and speed choice," in *Proc. 6th IEEE Int. Conf. Cognit. Infocommun. (CogInfoCom)*, Oct. 2015, pp. 343–347.

[33] T. Fontes, P. Fernandes, H. Rodrigues, J. M. Bandeira, S. R. Pereira, A. J. Khattak, and M. C. Coelho, "Are HOV/eco-lanes a sustainable option to reducing emissions in a medium-sized European city?" *Transp. Res. A, Policy Pract.*, vol. 63, pp. 93–106, May 2014.

[34] S. Kapoor, D. Grace, and T. Clarke, "A base station selection scheme for handover in a mobility-aware ultra-dense small cell urban vehicular environment," in *Proc. IEEE 28th Annu. Int. Symp. Pers., Indoor, Mobile Radio Commun. (PIMRC)*, Oct. 2017, pp. 1–5.

[35] Y. Aghazadeh, H. Kalbkhani, M. G. Shayesteh, and V. Solouk, "Cell selection for load balancing in heterogeneous networks," *Wireless Pers. Commun.*, vol. 101, no. 1, pp. 305–323, Jul. 2018.

[36] D. Bega, M. Gramaglia, C. J. B. Cano, A. Banchs, and X. Costa-Perez, "Toward the network of the future: From enabling technologies to 5G concepts," *Trans. Emerg. Telecommun. Technol.*, vol. 28, no. 8, p. e3205, Aug. 2017.

[37] J.-M. Moon and D.-H. Cho, "Novel handoff decision algorithm in hierarchical macro/femto-cell networks," in *Proc. IEEE Wireless Commun. Netw. Conf.*, Apr. 2010, pp. 1–6.

[38] A. Habibzadeh, S. S. Moghaddam, S. M. Razavizadeh, and M. Shirvanimoghaddam, "Analysis and performance evaluation of an efficient handover algorithm for cognitive HetNets," *Int. J. Commun. Syst.*, vol. 30, no. 16, p. e3315, Nov. 2017.

[39] A. Habibzadeh, S. S. Moghaddam, S. M. Razavizadeh, and M. Shirvanimoghaddam, "A novel handover decision-making algorithm for HetNets," in *Proc. IEEE Int. Symp. Signal Process. Inf. Technol. (ISSPIT)*, Dec. 2015, pp. 438–442.

[40] A. Habibzadeh, S. S. Moghaddam, S. M. Razavizadeh, and M. Shirvanimoghaddam, "Modeling and analysis of traffic-aware spectrum handover schemes in cognitive HetNets," *Trans. Emerg. Telecommun. Technol.*, vol. 28, no. 12, p. e3199, Dec. 2017.

[41] M. Ali, Q. Rabbani, M. Naeem, S. Qaisar, and F. Qamar, "Joint user association, power allocation, and throughput maximization in 5G H-CRAN networks," *IEEE Trans. Veh. Technol.*, vol. 66, no. 10, pp. 9254–9262, Oct. 2017.

[42] A. S. Cacciapuoti, "Mobility-aware user association for 5G mmWave networks," *IEEE Access*, vol. 5, pp. 21497–21507, 2017.

[43] Q. Zhang, J. Zeng, X. Su, L. Rong, and X. Xu, "Virtual small cell selection schemes based on sum rate analysis in ultra-dense network," in *Proc. Int. Conf. Commun. Netw. China*. Cham, Switzerland: Springer, 2016, pp. 78–87.
[44] M. Elkourdi, A. Mazin, and R. D. Gitlin, "Towards low latency in 5G HetNets: A Bayesian cell selection/user association approach," in *Proc. IEEE 5G World Forum (5GWF)*, Jul. 2018, pp. 268–272.
[45] M. Gharam and N. Boudriga, "Cell selection game in 5G heterogeneous networks," in *Proc. Int. Symp. Ubiquitous Netw.* Cham, Switzerland: Springer, 2018, pp. 28–39.
[46] B. R. Alyaei, I. M. Qureshi, S. Saleem, and S. H. Abbassi, "Offloading with hybrid cell association in non-uniform heterogeneous cellular networks: Modeling and performance analysis," *IEEE Access*, vol. 7, pp. 172214–172230, 2019.
[47] A. Alizadeh and M. Vu, "Load balancing user association in millimeter wave MIMO networks," *IEEE Trans. Wireless Commun.*, vol. 18, no. 6, pp. 2932–2945, Jun. 2019.
[48] J. Lee and Y. Yoo, "Handover cell selection using user mobility information in a 5G SDN-based network," in *Proc. 9th Int. Conf. Ubiquitous Future Netw. (ICUFN)*, Jul. 2017, pp. 697–702.
[49] D. S. Wickramasuriya, C. A. Perumalla, K. Davaslioglu, and R. D. Gitlin, "Base station prediction and proactive mobility management in virtual cells using recurrent neural networks," in *Proc. IEEE 18th Wireless Microw. Technol. Conf. (WAMICON)*, Apr. 2017, pp. 1–6.
[50] Q. Fan and N. Ansari, "Throughput aware and green energy aware user association in heterogeneous networks," in *Proc. IEEE Int. Conf. Commun. (ICC)*, May 2017, pp. 1–6.
[51] C. Xu, G. Zheng, and L. Tang, "Energy-aware user association for NOMA-based mobile edge computing using matching-coalition game," *IEEE Access*, vol. 8, pp. 61943–61955, 2020.
[52] M. Alhabo and L. Zhang, "Multi-criteria handover using modified weighted TOPSIS methods for heterogeneous networks," *IEEE Access*, vol. 6, pp. 40547–40558, 2018.
[53] M. Saimler and S. Coleri, "Multi-connectivity based uplink/downlink decoupled energy efficient user association in 5G heterogenous CRAN," *IEEE Commun. Lett.*, vol. 24, no. 4, pp. 858–862, Apr. 2020.
[54] W. Sun, L. Wang, J. Liu, N. Kato, and Y. Zhang, "Movement aware CoMP handover in heterogeneous ultra-dense networks," *IEEE Trans. Commun.*, vol. 69, no. 1, pp. 340–352, Jan. 2021.
[55] Y. Lu, M. Gerasimenko, R. Kovalchukov, M. Stusek, J. Urama, J. Hosek, M. Valkama, and E. S. Lohan, "Feasibility of location-aware handover for autonomous vehicles in industrial multi-radio environments," *Sensors*, vol. 20, no. 21, p. 6290, Nov. 2020.
[56] R. Duo, C. Wu, T. Yoshinaga, J. Zhang, and Y. Ji, "SDN-based handover scheme in cellular/IEEE 802.11p hybrid vehicular networks," *Sensors*, vol. 20, no. 4, p. 1082, Feb. 2020.
[57] K. M. Addali, S. Y. B. Melhem, Y. Khamayseh, Z. Zhang, and M. Kadoch, "Dynamic mobility load balancing for 5G small-cell networks based on utility functions," *IEEE Access*, vol. 7, pp. 126998–127011, 2019.
[58] D. Qu, Y. Zhou, L. Tian, and J. Shi, "User-centric QoS-aware interference coordination for ultra dense cellular networks," in *Proc. IEEE Global Commun. Conf. (GLOBECOM)*, Dec. 2016, pp. 1–6.
[59] "Technical specification group radio access network; study on channel model for frequencies from 0.5 to 100 GHz," Tech. Rep. 38.901, V16.1.0 (Release 16), 3GPP, 2019.
[60] R. El Banna, H. M. El Attar, and M. Aboul-Dahab, "Handover scheme for 5G communications on high speed trains," in *Proc. 5th Int. Conf. Fog Mobile Edge Comput. (FMEC)*, 2020, pp. 143–149.
[61] W. K. Lai, C.-S. Shieh, F.-S. Chou, C.-Y. Hsu, and M.-H. Shen, "Handover management for D2D communication in 5G networks," *Appl. Sci.*, vol. 10, no. 12, p. 4409, 2020.
[62] B. Banyassady, M. Korman, and W. Mulzer, "Computational geometry column 67," *ACM SIGACT News*, vol. 49, no. 2, pp. 77–94, 2018.
[63] A. Parkin, "Coordinate geometry," in *Digital Imaging Primer*. Berlin, Germany: Springer, 2016, pp. 61–77.
[64] I. A. M. García, "Astronomy, architecture and caverns," in *The Role of Archaeoastronomy in the Maya World: The Case Study of the Island of Cozumel*. Paris, France: UNESCO Publishing, 2016, p. 85.
[65] E. Ndashimye, N. I. Sarkar, and S. K. Ray, "A network selection method for handover in vehicle-to-infrastructure communications in multi-tier networks," *Wireless Netw.*, vol. 26, no. 1, pp. 387–401, 2020.
[66] X. Yan, Y. A. Sekercioglu, and N. Mani, "A method for minimizing unnecessary handovers in heterogeneous wireless networks," in *Proc. Int. Symp. World Wireless, Mobile Multimedia Netw.*, 2008, pp. 1–5.
[67] N. Han, S. Qiao, G. Yuan, R. Mao, K. Yue, and C.-A. Yuan, "A novel handover detection model via frequent trajectory patterns mining," *Int. J. Mach. Learn. Cybern.*, vol. 11, pp. 2587–2606, Apr. 2020.
[68] K. Chandra, A. S. Marcano, S. M. Mumtaz, R. V. Prasad, and H. L. Christiansen, "Unveiling capacity gains in ultradense networks: Using mm-wave NOMA," *IEEE Veh. Technol. Mag.*, vol. 13, no. 2, pp. 75–83, Jun. 2018.
[69] M. Elbayoumi, W. Hamouda, and A. Youssef, "Multiple-association supporting HTC/MTC in limited-backhaul capacity ultra-dense networks," *IEEE Trans. Commun.*, early access, Feb. 26, 2021, doi: 10.1109/TCOMM.2021.3062649.
[70] A. R. Elsherif, W.-P. Chen, A. Ito, and Z. Ding, "Adaptive resource allocation for interference management in small cell networks," *IEEE Trans. Commun.*, vol. 63, no. 6, pp. 2107–2125, Jun. 2015.
[71] H. Haci and A. Abdelbari, "Throughput enhanced scheduling (TES) scheme for ultra-dense networks," *Int. J. Commun. Syst.*, vol. 33, no. 4, p. e4229, 2020.

IBTIHAL AHMED ALABLANI received the B.S. degree in computer science from Princess Nourah Bint Abdulrahman University, in 2008, and the M.S. degree in computer engineering from King Saud University, in 2013, where she is currently pursuing the Ph.D. degree with the Computer Engineering Department. Since 2008, she has been working as a Faculty Member with Technical and Vocational Training Corporation (TVTC)/Technical College. Her research interests include wireless sensor networks, 5G heterogeneous networks, smart cities, and machine learning. She was awarded a Certificate of Excellence from the Saudi Ministry of Education as one of the top students in Saudi Arabia at high school, in 2004.

MOHAMMED AMER ARAFAH received the B.S. degree from King Saud University, Riyadh, Saudi Arabia, and the M.S. and Ph.D. degrees from the University of Southern California, Los Angeles, CA, USA. He is currently an Associate Professor of Computer Engineering with King Saud University. His research interests include computer network modeling and simulation, wireless sensor networks, cooperative relay networks, fault tolerance, 5G mobile communications, software-defined radios, multiple antenna systems, and high-speed networks.